

## ANCHORING OF CoHFC NANOPARTICLES ON CLINOPTILOLITE FOR REMEDY OF NUCLEAR WASTES

by

**Taher YOUSEFI<sup>1\*</sup>, Hamid Reza MAHMUDIAN<sup>2</sup>, Meisam TORAB-MOSTAEDI,  
Mohammad Ali MOOSAVIAN<sup>2</sup>, and Reza DAVARKHAH<sup>1</sup>**

<sup>1</sup>Nuclear Fuel Cycle Research School, Nuclear Science & Technology Research Institute, Tehran, Iran

<sup>2</sup>Department of Chemical Engineering, Faculty of Engineering, University of Tehran, Tehran, Iran

Scientific paper

<http://doi.org/10.2298/NTRP1701025Y>

To improve the mechanical properties, the cobalt ferrocyanide precipitation was carried out on clinoptilolite as an inorganic polymer. In this work the combination of two important factors, stability (zeolite) and high adsorption capacity (cobalt ferrocyanide) were considered to improve the ions uptake ability of adsorbent. The modification was approved by X-ray diffraction, Scanning electronic microscopy and Fourier transform infrared spectroscopy. The modified zeolite was applied to remove Sr(II) and Cs(I) ions from aqueous solution in a batch system. The adsorption capacities of modified zeolite for Cs(I) and Sr(II) improved to 90 and 130 mgg<sup>-1</sup>, respectively. The Sr(II) and Cs(I) removal were investigated as a function of shaking time, pH, Sr(II), and Cs(I) initial concentration and temperature. The experimental data were fitted well to Langmuir isotherm model for two sorbet metal ions. The time dependence sorption data showed that the uptakes of Cs(I) and Sr(II) were very rapid and apparent sorption equilibriums were achieved within 100 min of contact time. The kinetic experimental data were fitted to the pseudo-first order, pseudo-second order, the double exponential, Elovich and intraparticle diffusion models. The sorption rates and capacities as well as rate constants were evaluated.

*Key word:* natural zeolite, clinoptilolite, Cs(I), Sr(II), adsorption, cobalt ferrocyanide, nanoparticle

### INTRODUCTION

Synthetic and natural nanomaterials have been widely used as adsorbents, ion exchangers, molecular sieves and membranes [1-7]. Clinoptilolite, a widely available natural zeolite is crystalline, hydrated alkali and alkaline earth-aluminosilicate having an infinite, three dimensional, open structure [8]. The natural clinoptilolite with developed system of micro-pores aluminosilicate channels has a three-dimensional structure in which the channels are occupied by exchangeable ions and water [8, 9]. Based on the characters of alumino-silicate structure, three channel could be indicated in its framework. Two of the them are arranged in parallel to c axis and each other; a 10-member ring channel (tetrahedron) with size about of 4.4-7.2 Å (1 Å = 10<sup>-10</sup> m), and an 8-member ring channel with the size of 4.1-4.7 Å. Another channel with the size of 4.0-5.5 Å is a axis parallel channel consisting of an 8-member ring [9]. Zeolite's properties such as high surface area (due to larger channels), thermal, mechanical and chemical stability have attracted more

attention of researchers worldwide [10]. Radionuclides of Cs(I) and Sr(II), with great yield in the nuclear process and longer half-lives, are two of the most hazardous radioisotopes in the nuclear waste [11, 12]. Clinoptilolite has high affinity for removal of cation ions such as Cs(I) and Sr(II), however its capacity and selectivity can be improved by correct modification of zeolite surface by anchoring active functional groups on it [13-15]. For example, the cobalt ferrocyanide has a nanoporous framework with great guest-host interaction ability. The nanopores are occupied by alkaline cations (K<sup>+</sup>, Na<sup>+</sup>, *etc.*) and water molecules and they can be exchanged by other ions such as Cs(I), Sr(II) [16-18]. In other words cobalt ferrocyanides have shown a high selectivity for some metal ions and a large capacity. Moreover, they are effective over a wide pH range [16-19]. The major drawback of the ferrocyanides is associated which their nanometer or micrometer size that makes them available as fine powder, with low chemical and mechanical stability [16-19]. The metal hexacyanoferrates in the tiny powder form tend to aggregate, which reduces the high surface area to volume and causes high pressure drop or head loss in fixed-bed column operation.

\* Corresponding author; e-mail: [taher\\_yosefy@yahoo.com](mailto:taher_yosefy@yahoo.com)

These are not suitable for any flow-through systems and subsequently reduce their effectiveness [16-19].

For this reason, many techniques have been designed for immobilizing of these adsorbent on suitable matrices that can be organic (mainly polymers and biopolymers) or inorganic (mineral) supports: In other words, to improve the mechanical properties of ferrocyanides, they are prepared by precipitation on solid inert supports such as mineral (zeolites and silica gels) and organic carbon-based matrices [19]. This immobilization may proceed by *in situ* entrapment/encapsulation. The inorganic matrices are more suitable for corrosive and radioactive materials [9]. Natural clinoptilolite, with micro-pores can be used as a carrier of metal ferrocyanides nanoparticles as a mineral supporter [8-10]. As mentioned above clinoptilolite is a selective ion-exchanger for alkali and rare alkali metal ions and has a relatively large sorption capacity, and cobalt ferrocyanide has a nanoporous framework with great guest-host interaction ability for alkali and rare alkali metal ions [special Cs(I)]. In this work, the strategy was the synthesis of an adsorbent with high stability and capacity, therefore, the cobalt cyanoferrates nanoparticles were synthesized on an inorganic supporter, namely natural clinoptilolite zeolite. In fact, the combination of the two important factors: stability (zeolite) and high adsorption capacity (cobalt ferrocyanide) was considered to improve the metal ions adsorption ability of the adsorbent.

## EXPERIMENTAL

### Materials and characterization

The materials such as hydrochloric acid,  $\text{CoCl}_2 \cdot 6\text{H}_2\text{O}$ ,  $\text{K}_3\text{Fe}(\text{CN})_6$ ,  $\text{Cs}(\text{NO}_3)$  and  $\text{Sr}(\text{NO}_3)_2$  were obtained from Merck and used without further purification. The solutions were prepared by distilled water. Iranian natural zeolite used in this study, was supplied from mining companies. Ball milling of the zeolites was performed by means of a planetary ball mill (NARYA MPM 4\*250, Amin Asia Fanavar Pars, IRAN). The characterization of natural and modified zeolite was done by scanning electron microscopy (SEM), (LEO 1455VP), X-ray diffraction (XRD, Phillips, PW-1800) equipped with monochromatized Cu K $\alpha$  radiation ( $k = 0.154$  nm, 40 kV, and 30 mA), Fourier Transform Infrared of samples were recorded with a KBr pellet on a VECTOR-22 (Bruker) spectrometer ranging from 400 to 4000  $\text{cm}^{-1}$ .

### Zeolite modifying

The natural zeolite was modified in the presence of potassium hexacyanoferrate and cobalt nitrate respectively. 5 g of the powdered clinoptilolite dried at 150 °C

was added to a 100 mL solution of 0.1 M  $\text{Co}(\text{NO}_3)_2$  under continuous string condition at 25 °C for 2 hours. After filtering, the zeolite was washed with deionized water and mixed with a 100 mL of 0.1 M  $\text{K}_4\text{Fe}(\text{CN})_6$  solution to form CoHCF precipitates in the micropores of clinoptilolite. The loaded zeolite was then washed with deionized water and dried at 60 °C (Behdad Drying Oven, 01 145, IRAN) for 2 hours.

### Cs(I) and Sr(II) sorption

The Cs(I) and Sr(II) ions uptake was determined in batch adsorption mode using 0.1 g of adsorbent with 20 ml of solutions with continuous stirring. After the enough mixing time, the filtration was performed and AAS and ICP techniques were used to determine the remained  $\text{Cs}^+$  and  $\text{Sr}^{2+}$  in the filtered solution. The uptake degree is defined as

$$q_e = (C_i - C_e) \frac{V}{w} \quad (1)$$

where  $C_i$  ( $\text{mg L}^{-1}$ ) and  $C_e$  ( $\text{mg L}^{-1}$ ) are the initial and final metal ions concentrations in solution respectively,  $w$  [g] is the solid phase mass and  $V$  [L] is the volume.

The uptake percentage was determined as follows

$$\text{Adsorption} = \frac{c_i - c_e}{c_i} 100 \text{ [\%]} \quad (2)$$

The influences of contact time, initial concentration, pH and temperature parameters were studied to evaluate the modified zeolite characteristics and the adsorption thermodynamic parameters.

## RESULTS AND DISCUSSION

### Zeolite modification

Our investigation revolves around natural clinoptilolite, with micro-pores which was used as a carrier of metal ferrocyanides nanoparticles as a mineral support [20]. Potassium cobalt hexacyanoferrate particles were incorporated in the porous matrix of zeolites by successive impregnation with  $\text{Co}(\text{NO}_3)_2$  and  $\text{K}_4\text{Fe}(\text{CN})_6$ . In fact, mechanical stability and high surface area of clinoptilolite are combined with high adsorption capacity and selectivity of cobalt ferrocyanide to obtain an improved adsorbent.

The replacement of  $\text{Si}^{4+}$  by  $\text{Al}^{3+}$  in tetrahedral positions of crystal produces non-compensated negative charges that this non-compensated negative charge and the surface functional groups in the zeolite are responsible of ion exchange property of zeolite [21-23]. It is well known that cobalt ferrocyanide crystal includes  $\text{K}^+$ ,  $\text{Na}^+$  or  $\text{Ca}^{2+}$  ions, which play an important role in the uptake of the metal ions.

### Fourier transform infrared spectroscopy and X-ray diffraction

The Fourier transform infrared spectroscopy (FT-IR) spectra of the bare and modified zeolites were investigated in the 4000-400  $\text{cm}^{-1}$  region, fig. 1(a). Peaks at 1060  $\text{cm}^{-1}$ , 794  $\text{cm}^{-1}$ , and 609  $\text{cm}^{-1}$  were characteristic of clinoptilolite [24]. The strongest band observed at 1060  $\text{cm}^{-1}$  was assigned to the asymmetric internal tetrahedral bending. The second strongest band at 465  $\text{cm}^{-1}$  corresponded to the internal bending. The band observed at 609  $\text{cm}^{-1}$  was related to the presence of double rings in the framework structure. Other bands at 1208  $\text{cm}^{-1}$ , 790  $\text{cm}^{-1}$ , and 711  $\text{cm}^{-1}$  were assigned to the asymmetric stretching modes of internal tetrahedra, symmetric stretching of external tetrahedra and symmetric stretching of internal tetrahedra, respectively. The 670  $\text{cm}^{-1}$  band arises from symmetric tetrahedral stretching [25]. In modified zeolite, a sharp peak at 2090  $\text{cm}^{-1}$ , is a characteristic of the C≡N group and it confirms the presence of cobalt ferrocyanide in the zeolite [26]. The X-ray diffraction (XRD) patterns of bare zeolite and cobalt ferrocyanide loaded zeolite are shown in fig. 1(b). The XRD pattern showed the characteristic reflection peaks at Bragg angle ( $2\theta$ ) = 10°, 11.3°, 13.2°, 22.5°, 27°, 30.02°, and 32°, respectively. The pattern indicates that the natural

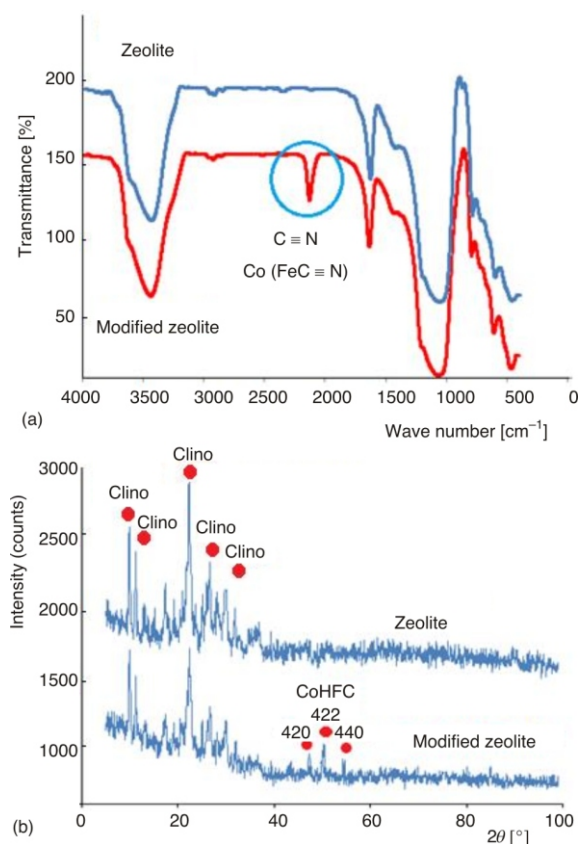


Figure 1. FT-IR spectra (a) and XRD patterns (b) of bare and CoHFC loaded zeolites

zeolite used in this study was classified into clinoptilolite [25]. Clinoptilolite with the ideal formula of  $(\text{Na}, \text{K})_6 \text{Si}_{30}\text{Al}_6\text{O}_{72} \cdot n\text{H}_2\text{O}$  is the most common natural zeolite found mainly in sedimentary rocks of volcanic origin [24]. The XRD pattern of CoHCF modified zeolite in addition to the characteristic peaks of clinoptilolite shows characteristic peaks at  $2\theta = 40^\circ$ ,  $50^\circ$ , and  $55^\circ$  correspond to 420, 422, and 440 plane of the crystal structure of cobalt hexacyanoferrate (JCPDS card no: 46907) [27].

### Scanning electron microscopy

To determine the surface morphology and particle size of the natural and modified zeolites, the scanning electronic microscopy (SEM) analysis was performed. Figure 2 shows the SEM images of the samples in two different magnifications. As can be seen the SEM images reveal that the morphology of the samples is approximately the same and the product comprises large clusters formed from the sub-grain irregular particles with the average size of about 50 nm. However, a careful and detailed look at the images of modified zeolite indicates that the fine nano structures are interconnected to each other giving a porous and rod-like (diameter about 15 nm) appearance to the morphology.

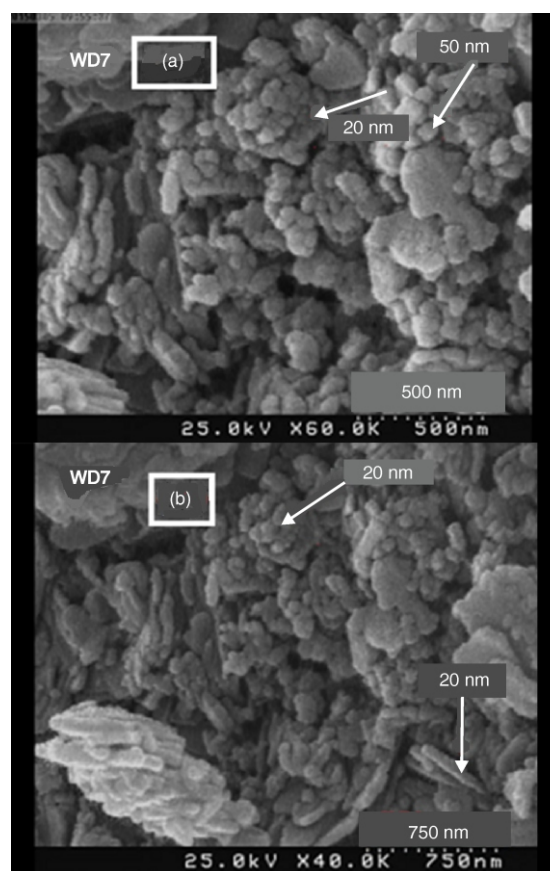
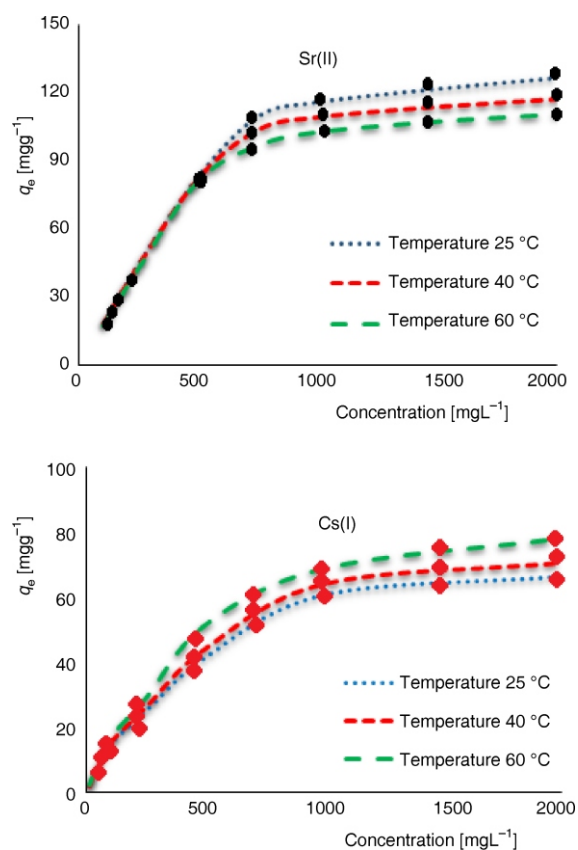


Figure 2. SEM images of (a) bare zeolite, (b) modified zeolites

## Sr(II) and Cs(I) uptake

### Effect of temperature and initial concentration

The Sr(II) and Cs(I) sorptions at different initial concentrations of 10, 25, 75, 50, 100, 250, 500, 750, 1000, 1500, and 2000  $\text{mgL}^{-1}$  and different temperatures of 298, 313, and 333  $^{\circ}\text{C}$  in contact time of 120 min and  $\text{pH} = 6.5$  were studied to realize the relation between the uptake amount vs. concentration and temperature, (fig. 3). As shown, in concentration range of 10 to 1000 ppm, the removal (sorption) increased by the increasing the metal ion concentration, but the sorption became constant at higher concentration. Mass transfer at the aqueous and the solid interfaces and probability of collision between ions and the adsorbent active sites are important factors which increase the adsorption capacity at higher concentration. The higher ions concentration supplied a driving force to vanquish the mass transfer wall at solid and aqueous interfaces and a higher probability of collision between each investigated ion and the adsorbent particles [13, 19]. Initially, all active sites of the adsorbent are vacant and the metal ion concentration gradient is relatively high, causing high sorption. With increasing ion concentration, the saturation of the active sites leads to a decrease in the available position for interaction with metal ions (plateau represents). These results



**Figure 3. Effect of initial Sr(II) and Cs(I) ion concentrations on the amount of sorption**

indicate that energetically less favorable sites become involved in increasing metal concentration in the aqueous solution. The obtained results shows that the uptake capacities of unmodified zeolite were about 58 and 109  $\text{mgg}^{-1}$  which they reached to about 90 and 130  $\text{mgg}^{-1}$  after modification for Cs(I) and Sr(II) respectively.

Effect of the temperature can also be seen in fig. 3. The results show that the increase in temperature has a positive effect on the uptake of Cs(I) ions and a negative uptake effect of Sr(II) ions. The metal ion uptake process can be affected by temperature through diverse ways. Higher sorption capacity can be achieved by increasing of temperature through decreasing of solution viscosity and increasing of diffusion coefficient of ions in boundary layer of the adsorbent. The equilibrium sorption capacity of the adsorbent would be effected by the change of temperature. For instance, the adsorption capacity will decrease upon increasing the temperature for an exothermic reaction and will increase for an endothermic one. Furthermore, the adsorbent sites will be more active at higher temperatures. In fact, the ions kinetic energy increases at elevated temperatures, thus, the probability the effective contact between ions and the active site increases, and adsorption efficiency increases consequently. Three thermodynamic parameters including free energy ( $G^{\circ}$ ), enthalpy ( $H^{\circ}$ ), and entropy ( $S^{\circ}$ ) were determined by considering the thermodynamic equilibrium constants. The  $G^{\circ}$  was determined through the following equation.

$$\Delta G = RT \ln K \quad (3)$$

where  $G^{\circ}$  is the standard free energy change,  $R$  – the gas constant ( $8.314 \text{ Jmol}^{-1}\text{K}^{-1}$ ),  $T$  – the temperature, and  $K$  – the equilibrium constant of the sorption process. The values of  $K$  were obtained according to the following equation

$$K = \lim_{C_e \rightarrow 0} \frac{C_e}{C_{e1}} \quad \text{or} \quad K = \frac{q_e}{C_e} \quad (4)$$

where  $C_{e1}$  and  $C_{e_s}$  [ $\text{mgL}^{-1}$ ] are the equilibrium concentration of the ions in the liquid and the solid phase respectively.

The slope and intercept of Van't Hoff graph ( $\ln K$  vs.  $1/T$ ) were used for determination of enthalpy ( $H^{\circ}$ ) and entropy ( $S^{\circ}$ ) changes (fig. 4), by the following equation [22, 23]

$$\ln K = \frac{\Delta S^{\circ}}{R} - \frac{\Delta H^{\circ}}{R} \frac{1}{T} \quad (5)$$

The calculated thermodynamic parameters are listed in tab. 1. As shown in fig. 4 and from the  $R^2$  values, the linearity of the  $\ln K$  vs.  $1/T$  plot is satisfactory.

The negative value of standard free energy ( $G^{\circ}$ ) showed that the uptake processes of Sr(II) and Cs(I) are thermodynamically spontaneous. The de-

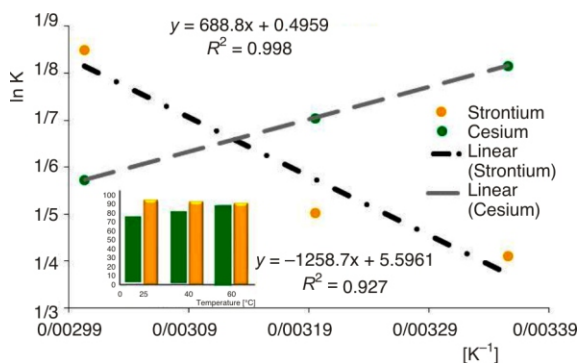


**Figure 4.** Plot of  $\ln K$  vs.  $1/T$  for estimation of thermodynamic parameter

**Table 1.** Thermodynamic parameters for adsorption of Sr(II) and Cs(I)

Metal	$H^\circ$ [kJmol <sup>-1</sup> ]	$S^\circ$ [Jmol <sup>-1</sup> K <sup>-1</sup> ]	$G^\circ$ [kJmol <sup>-1</sup> ]		
			298 K	313 K	333 K
Sr(II)	10.4648	46.526	-3.3999	-4.0978	-5.0283
Cs(I)	-5.7266	-4.1229	-4.4980	-4.4362	-4.3537

crease in  $G^\circ$  values with an increase in temperatures for Sr(II) indicates desirable uptake (sorption) at higher temperatures. For Cs(I) sorption process the standard free energy ( $G^\circ$ ) increase with an increase in temperatures shows an undesirable sorption at higher temperatures. Table 1 indicates that the uptake of Cs<sup>+</sup> by the modified zeolite is an exothermic nature (the negative values of  $H^\circ$ ). In other word the negative value of the  $H^\circ$  shows a strong binding between the adsorbate ions and the modified zeolite and high affinity of modified zeolite to Cs<sup>+</sup> ions.

The sorption capacity decreases with increasing of temperature due to exothermic behavior of sorption process [19, 28]. The negative value of  $S$  indicates the intercalation of Cs<sup>+</sup> inside cobalt ferrocyanide cage leading to more stabilization of the Cs<sup>+</sup> ions. In other words, immobilization of cesium ions contributes to a decrease in the freedom of the adsorbate ions and thus negative entropy. The enthalpy ( $H^\circ$ ) value of the Sr<sup>2+</sup> uptake is positive which indicates the Sr<sup>2+</sup> adsorption is endothermic and increases with increasing of temperature.

The immobilization of Sr<sup>2+</sup> ions on the surface of the modified zeolite led to liberation of more ions ( $K^+$ ) and positive entropy value. In addition, the positive value of entropy can be attributed to increasing of randomness at the solid-liquid interface during the sorption of Sr<sup>2+</sup> ion on the active sites of the modified zeolite [13-19].

*Effect of pH*

The pH in solutions can either suppress or promote the adsorption of metal ions with altering the metal ion forms in solution and the adsorbent surface properties. Figure 5 shows the effect of pH upon the

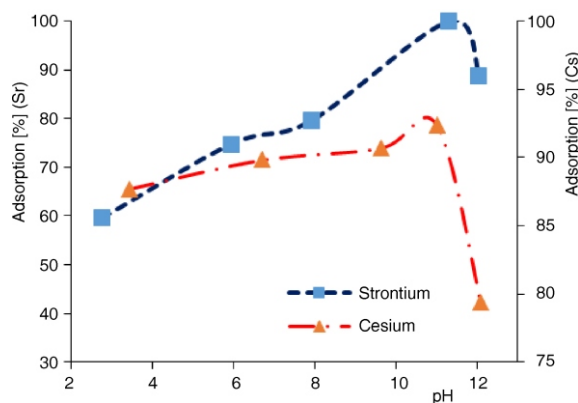


**Figure 5.** Effect of pH on Sr(II) and Cs(I) sorption on modified zeolite

removal of Cs(I) and Sr(II) at initial concentration of Co(Sr) = Co(Cs) = 150 mgg<sup>-1</sup> by modified zeolite at pH of 2.5, 5.5, 7.5, 11, and 12 (in 120 min contact time and 298 K). Evidently, the Cs(I) removal by the adsorbent does not show any important change in 2-11 pH range but a serious decrease in the uptake with increasing pH to 12.0. At alkaline pH, hydrolysis (slightly) of cesium and strontium ions and the dissolution (mainly) of sorbent are responsible for the decrease in the uptake capacity [29-31]. When the pH is low (pH 2), the adsorbent barely shows any affinity with Sr(II) ions. Thus, the strong acidity results in replacing the adsorbed Sr(II) ions by the H<sup>+</sup>, consequently decreasing the adsorption capacity of Sr(II) ions [29, 30].

*Time effect*

The sorption kinetics parameters can be determined by varying the contact time between the sorbent and metal ions, fig. 6. The time-dependent behaviors of Sr(II) and Cs(I) ions adsorption, were measured by varying the equilibrium time (15, 30, 60, 120, 240, and 480 min) at initial concentration of C<sub>0</sub>(Sr)150 mgg<sup>-1</sup> and Co(Cs)100 mgg<sup>-1</sup>, pH = 6.5 and 298 K. The results showed that the ions removal process is characterized by a fast adsorption in the initial contact time and equilibrium in the next 100 min. Firstly, large metal ions

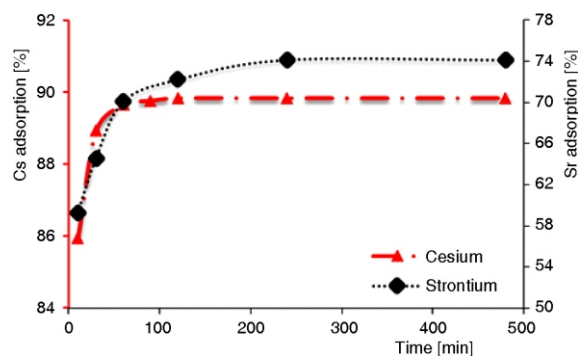


**Figure 6.** Effect of contact time on Sr(II) and Cs(I) adsorptions on modified zeolite

concentration gradient between sorbent and the solution led to fast uptake of ions and achievement of 90% the equilibrium capacity [13, 19]. Later, the adsorption slowed down possibly because more sorption sites were occupied [13, 19]. Then, the equilibrium was achieved and no change in sorption capacity was shown. The kinetic factors, give significant information for modeling and designing the adsorption processes. The kinetic parameters were extracted from fitting of obtained experimental data with kinetic models. Thus, the pseudo first-order, pseudo-second-order model, the double exponential model, Elovich model and intraparticle diffusion were the equations used to fit the experimental data (fig. 7). The correlation coefficients ( $R^2$ ) were used to determine adaptation between the experimental data and the models (tab. 1). In order to describe the rate-limiting steps of the removal process and to determine intraparticle diffusion coefficients for the modified zeolite, the sorption kinetics data were fitted to a diffusion model.

The earliest equation describing the adsorption rate of an adsorbate from a liquid phase is the pseudo-first-order rate expression. It is represented as [19]

$$\frac{dq}{dt} = K_1(q_e - q) \quad (6)$$

where  $q_e$  [ $\text{mgg}^{-1}$ ] is the value of the adsorbed ions in equilibrium condition and  $q_t$  [ $\text{mgg}^{-1}$ ] is the value of the adsorbed ions at time  $t$  on the modified zeolite, and  $K_1$  [ $\text{min}^{-1}$ ] is rate constant of the adsorption. Integrating (eq. 4) under the special (boundary) conditions of  $q_t = 0$  at  $t = 0$  and  $q_t = q_t$  at  $t = t$ , gives

$$\ln(q_e - q_t) = \ln q_e - K_1 t \quad (7)$$

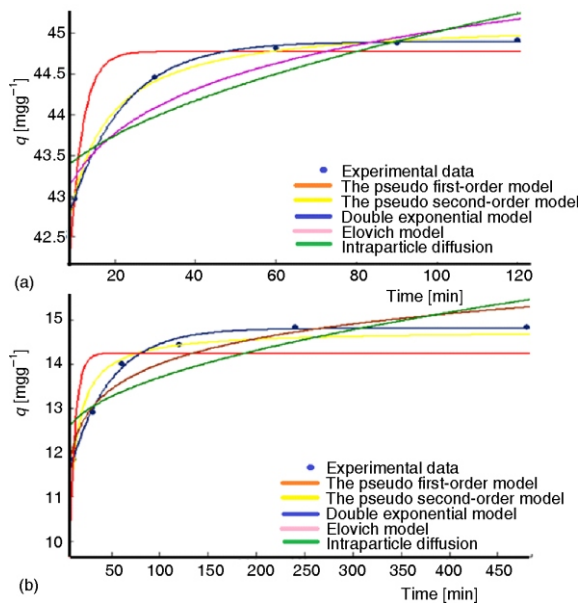


**Figure 7.** Kinetic models plots for the sorption of (a) Cs(I) and (b) Sr(II) ions from aqueous solutions onto modified zeolite

**Table 2.** Kinetic parameters for Cs(I) sorption by modified zeolite

Kinetic models	Parameter	Value
The pseudo first-order model	$k_2$ [ $\text{min}^{-1}$ ]	0.3211
	$q_e$ [ $\text{mgg}^{-1}$ ]	44.77
	$R^2$	0.8129
The pseudo second-order model	$k_2'$ [ $\text{gmg}^{-1}$ ]	0.04388
	$q_e$ [ $\text{mgg}^{-1}$ ]	45.16
	$h$ [ $\text{mgg}^{-1}\text{min}$ ]	89.49
	$R^2$	0.917
Double exponential model	$D_1$ [ $\text{mgL}^{-1}$ ]	20.2
	$D_2$ [ $\text{mgL}^{-1}$ ]	0.1313
	$K_{D1}$ [ $\text{min}^{-1}$ ]	0.9997
	$K_{D2}$ [ $\text{min}^{-1}$ ]	0.07427
	$q_e$ [ $\text{mgg}^{-1}$ ]	44.89
	$R^2$	0.9995
Intraparticle diffusion	$k_{id}$ [ $\text{mgg}^{-1}\text{min}^{0.5}$ ]	0.2304
	Intercept [C]	42.71
	$R^2$	0.8542
Elovich model	$\alpha$ [ $\text{mgg}^{-1}\text{min}^{-1}$ ]	0.7813
	$\beta$ [ $\text{mgg}^{-1}$ ]	41.43
	$R^2$	0.9245

or

$$q_t = q_e(1 - e^{-K_1 t}) \quad (8)$$

From the intercept and slope of the  $\ln(q_e - q_t)$  vs. time ( $t$ ) graph of the  $q_e$  and  $K_1$  can be determined (eq. 7)

The pseudo second-order rate kinetic model was used to explain the sorption of Sr(II) and Cs(I) ions onto the modified zeolite. The second-order rate kinetic model is as [13, 19]

$$\frac{dq_t}{dt} = k_2(q_e - q_t)^2 \quad (9)$$

The integrated form of eq. (9) under the special conditions (boundary condition:  $t=0$  to  $t=t$  and  $q_t=0$  to  $q_t=q_t$ ) is as

$$\frac{1}{q_e - q_t} - \frac{1}{q_e} = k_2 t \quad (10)$$

$$\frac{t}{q_t} = \frac{1}{k_2 q_e^2} + \frac{1}{q_e} t \quad (11)$$

The  $k_2$  [ $\text{gmg}^{-1}\text{min}$ ] is the rate constant of the pseudo-second-order model.

The  $h$  [ $\text{mgL}^{-1}$ ]; initial sorption rate  $h$  ( $\text{mgL}^{-1}\text{h}$ ) is as

$$h = k_2 q_e^2 \quad (12)$$

then eqs. (11) and (12) become

$$\frac{t}{q} = \frac{1}{h} + \frac{1}{q_e} t \quad (13)$$

The kinetic parameters were extracted from the graph of the  $t/q_t$  vs.  $t$ . The correlation coefficient ( $R^2$ ) determines conformity between the parameters and experimental data.

The mathematical equation of intraparticle diffusion kinetic model is as [24]

$$q_t = k_{ad} t^{1/2} + c \quad (14)$$

where  $k_{ad}$  is the rate constant of intraparticle transport [ $\text{mgg}^{-1} \text{min}^{1/2}$ ], and  $c$  – the boundary layer diffusion. Pursuant to the intraparticle diffusion kinetic model, plotting of  $q_t$  vs.  $t^{1/2}$ , in shadow of the straight line with intercept  $c$ , confirms that the involved mechanism is a diffusion of the species. The Elovich model which explains the sorption rate decreases exponentially with increases of sorbent amount is as [32]

$$\frac{dq}{dt} = \alpha e^{-\alpha q} \quad (15)$$

where  $q$  represents the amount of ions adsorbed at time  $t$ , the desorption constant, and  $\alpha$  the initial adsorption rate. The Elovich equation has been used to describe the adsorption process of pollutants from aqueous solutions. Another model which was used to describe Sr(II) and Cs(I) adsorptions was double-exponential. The double-exponential model is as

$$q_t = q_e \left[ \frac{D_1}{m_{ads}} \exp(-K_{D_1} t) + \frac{D_2}{m_{ads}} \exp(-K_{D_2} t) \right] \quad (16)$$

The  $D_1$  [ $\text{mgL}^{-1}$ ] and  $D_2$  [ $\text{mgL}^{-1}$ ] coefficients are the rapidly and slowly adsorbed fractions value of ion, respectively. The  $K_{D_1}$  [ $\text{min}^{-1}$ ] and  $K_{D_2}$  [ $\text{min}^{-1}$ ] are rate constants of the rapid and slow steps. The slow and rapid steps extracted parameters (from the experimental data) are given in tabs. 2 and 3. The extracted kinetic parameters of five kinetic models and the correspond correlation coefficients ( $R^2$ ) are presented in tabs. 2 and 3. These data, evidently disclose, that the correlation coefficient ( $R^2$ ) has a high value and is closer to unity for the double-exponential kinetic model than the other kinetic model for Cs(I) and Sr(II), thus clarifying the matching of the experimental data by the double-exponential kinetic model. Based on this model, the uptake process of ions could be adopted in two steps, first namely a rapid phase involving external and internal diffusions, and second namely a slow phase controlled by the intraparticle diffusion. As can be seen  $D_1 = 20.2$  and  $D_2 = 0.1313$  are the amounts of rapidly and slowly adsorbed fractions of Cs(I) ion [ $\text{mgL}^{-1}$ ], respectively, and  $K_{D_1} = 0.9997$  and  $K_{D_2} = 0.07427$  are rapid and slow rate constants [ $\text{min}^{-1}$ ] of Cs(I). Also for Sr(II) ions these constants are:  $D_1 = 18.82$  and  $D_2 = 0.0001$  and  $K_{D_1} = 0.9997$  and  $K_{D_2} = 0.07427$ . As can be seen,  $D_1$  and  $K_{D_1}$  are greater than  $D_2$  and  $K_{D_2}$ , respectively. Rapidly and slowly adsorbed fractions [%],  $RF$  and  $SF$ , can be calculated as

$$RF = 100 \frac{D_1}{D_1 + D_2} \quad RF_{Cs} = 99.3 \quad RF_{Sr} = 99.99$$

$$SF = 100 \frac{D_2}{D_1 + D_2} \quad SF_{Cs} = 0.7 \quad SF_{Sr} = 0.01$$

**Table 3. Kinetic parameters for Sr(II) sorption by modified zeolite**

Kinetic models	Parameter	Value
The pseudo first-order model	$k_1$ [ $\text{min}^{-1}$ ]	0.1733
	$q_e$ [ $\text{mgg}^{-1}$ ]	14.25
	$R^2$	0.6709
The pseudo second-order model	$k'_2$ [ $\text{gmg}^{-1}$ ]	0.02465
	$q_e$ [ $\text{mgg}^{-1}$ ]	14.76
	$h$ [ $\text{mgg}^{-1} \text{min}$ ]	5.3701
	$R^2$	0.9258
Double exponential model	$D_1$ [ $\text{mgL}^{-1}$ ]	18.82
	$D_2$ [ $\text{mgL}^{-1}$ ]	0.0001
	$K_{D1}$ [ $\text{min}^{-1}$ ]	2
	$K_{D2}$ [ $\text{min}^{-1}$ ]	0.02387
	$q_e$ [ $\text{mgg}^{-1}$ ]	14.8
	$R^2$	0.9947
Intraparticle diffusion	$k_{id}$ [ $\text{mgg}^{-1} \text{min}^{0.5}$ ]	0.1466
	Intercept [C]	12.23
	$R^2$	0.7803
Elovich model	$\alpha$ [ $\text{mgg}^{-1} \text{min}^{-1}$ ]	0.8162
	$\beta$ [ $\text{mgg}^{-1}$ ]	10.25
	$R^2$	0.9295

The obtained data indicated that the metal ions sorption onto the sorbent initially occurred within a fast removal rate stage, followed by a second slower removal rate stage, until reaching equilibrium. In other words in sorption process, more than 90 % of the total process completed was achieved in initial stage, and in the second stage, equilibrium attained in the second stage. It was also suggested that in the first stage which was faster than the second stage, the metal ions were accumulated in the large available surface of sorbent. The sorption process was slowed down with the gradual occupation of surface binding sites [33].

The best fitted kinetic models determined by correlation coefficients ( $R^2$ ) are found to be in the order of: Double exponential model > Elovich model = Pseudo second-order model. Adsorption isotherms explain the relation between the adsorbate concentration in the bulk solution and the adsorbed amount at the solid/liquid interface. The Langmuir, Freundlich, Dubinin-Radushkevich, and Temkin isotherm models are the most used models to explanation equilibrium adsorption isotherms and calculation of adsorption parameters [34]. The Sr(II) and Cs(I) solutions with different concentrations were utilized for the adsorption isotherm investigation. A valid model for monolayer adsorption on a surface with a finite number of identical sites, is Langmuir model, which can be expressed as [35, 36]

$$\frac{C_e}{q_e} = \frac{1}{q_m K} + \frac{C_e}{q_m} \quad (17)$$

where  $q_m$  [ $\text{mgg}^{-1}$ ] is the maximum removal capacity (monolayer),  $C_e$  – the equilibrium concentration of the metal ion in the equilibrium solution [ $\text{mgL}^{-1}$ ], and  $K$

[ $\text{Lmg}^{-1}$ ] – the Langmuir constant related to the free energy of adsorption ( $b = e^{G/RT}$ ). The non-ideal and reversible adsorption in multilayer would be described by Freundlich isotherm, and the linear form of the equation [37]

$$\ln(q_e) = \ln(K_p) + \frac{1}{r} \ln(C_e) \quad (18)$$

where  $C_e$  [ $\text{mgL}^{-1}$ ] is the equilibrium concentration of ions,  $q_e$  [ $\text{mgg}^{-1}$ ] – the amount of adsorbed ions,  $n$  and  $K_F$  [ $\text{mgg}^{-1}$ ] – the Freundlich constants related to the intensity of the adsorption and the sorption capacity respectively. In the Temkin isotherm, the interactions between the adsorbed species are not ignored and enthalpy of all the adsorbed molecules in solution is accomplished [38]. The Temkin isotherm is as

$$q_e = B \ln A_T + B \ln C_e \quad (19)$$

where  $B$  [ $\text{Jmol}^{-1}$ ] and  $A_T$  [ $\text{Lg}^{-1}$ ] are, the constants related to the sorption heat and Temkin isotherm equilibrium binding respectively. From the slope and intercept of  $q_e$  vs.  $\ln C_e$  curve the constants could be determined. The extremely high and low concentration values are ignored in the Temkin isotherm. This model considers linear of decrease of the molecules adsorption heat rather than logarithmic coverage.

The Dubinin-Radushkevich ( $D-R$ ) isotherm is similar to Langmuir isotherm, but it does not assume a homogeneous surface or constant sorption potential [39-41]. This empirical model is useful to understand the pore-filling mechanism in high and intermediate concentration ranges (it deviates at lower concentration). The  $D-R$  isotherm is as the following

$$\ln q_e = \ln q_m - B_{DR} \xi^2 \quad (20)$$

where  $q_m$  is the maximum of sorbed ion by adsorbent [ $\text{mmolk}^{-1}$ ],  $B_{DR}$  – a constant related to the sorption energy [ $\text{mol}^2\text{kJ}^{-2}$ ], and  $\xi$  – the Polanyi potential ( $RT \ln(1 + 1/C_e)$ ), where  $R$  and  $T$  are the gas constant [ $\text{kJmol}^{-1}\text{K}^{-1}$ ], the absolute temperature respectively. The  $\xi$  is equal to eq. (21)

$$\xi = RT \ln \left( 1 + \frac{1}{C_e} \right) \quad (21)$$

where  $C_e$  is the adsorbate equilibrium concentration [ $\text{mgL}^{-1}$ ].

Figure 8(a-h) shows the adsorption isotherms of Sr(II) and Cs(I) ions on the modified zeolite. Langmuir, Freundlich, Temkin, and Dubinin-Radushkevich constants and the coefficients, are listed in tab. 4.

Evidently, the data fit well with Langmuir and Dubinin-Radushkevich ( $D-R$ ) isotherms. Langmuir model can give an insight to the maximum uptake capacity and indicate whether the sorption is favorable or not. The  $q_m$  and  $K$  were determined from the slope and intercept of the  $C_e/q_e$  vs.  $C_e$  curve in Langmuir

model. Table 4, indicates that the  $R^2$  value approaches one as the temperature value is increased, and it means that the adsorption of Cs(I) and Sr(II) ions onto modified zeolite is more compatible with these models at high temperature of the solution. According to the results, acceptable agreement between the calculated (obtained from the Langmuir equation) and experimental values of adsorption capacity can be seen.

The Dubinin-Radushkevich data in tab. 4, would be used to determine nature of sorption process.  $B_{DR}$  is a constant related to the sorption energy [ $\text{mol}^2\text{kJ}^{-2}$ ], and  $E_a$  is free energy of sorption per molecule of the sorbate when it is transferred to the surface of the solid from infinity in solution

$$E = \frac{1}{\sqrt{2K_{ad}}}$$

where  $K_{ad}$  is denoted as the isotherm constant.  $E_a$  value can be used to determine the sorption mechanism of ions removal.

## CONCLUSION

The most common natural zeolite is clinoptilolite. Clinoptilolite is characterized by cage-like structures, high surface areas and cation exchange property. Treatment of clinoptilolite with cobalt ferrocyanide dramatically alters its surface chemistries and improves its cation uptake capacity. The present study focuses on modification of clinoptilolite with cobalt ferrocyanide and adsorption of Cs(I) and Sr(II) from aqueous solutions using the obtained modified zeolite as a low-cost sorbent. The modification process was approved by XRD, FTIR, and SEM analyses and then tested as an adsorbent for the uptake of Cs(I) and Sr(II) ions from aqueous solutions. The ion uptake characteristic has been examined by the variations in the parameters of concentration of the metal ions, pH, contact time, and temperature. The SEM images of the product showed that it consists of particles with sizes ranging from 10 to 90 nm. The adsorption capacities of bare zeolite for Cs(I) and Sr(II) removal were about 58 and 109  $\text{mgg}^{-1}$ , respectively, and the adsorption capacities of modified zeolite for Cs(I) and Sr(II) removal were about 90 and 130  $\text{mgg}^{-1}$ , respectively. The kinetic results demonstrated that the uptake of Cs(I) and Sr(II) ions from the solution by modified zeolite reached equilibrium within 100 min and was governed by double-exponential kinetic model. Obviously, this adsorbent has effective removal properties for the adsorption of Cs(I) Sr(II) from the radioactive waste compared with other adsorbents.

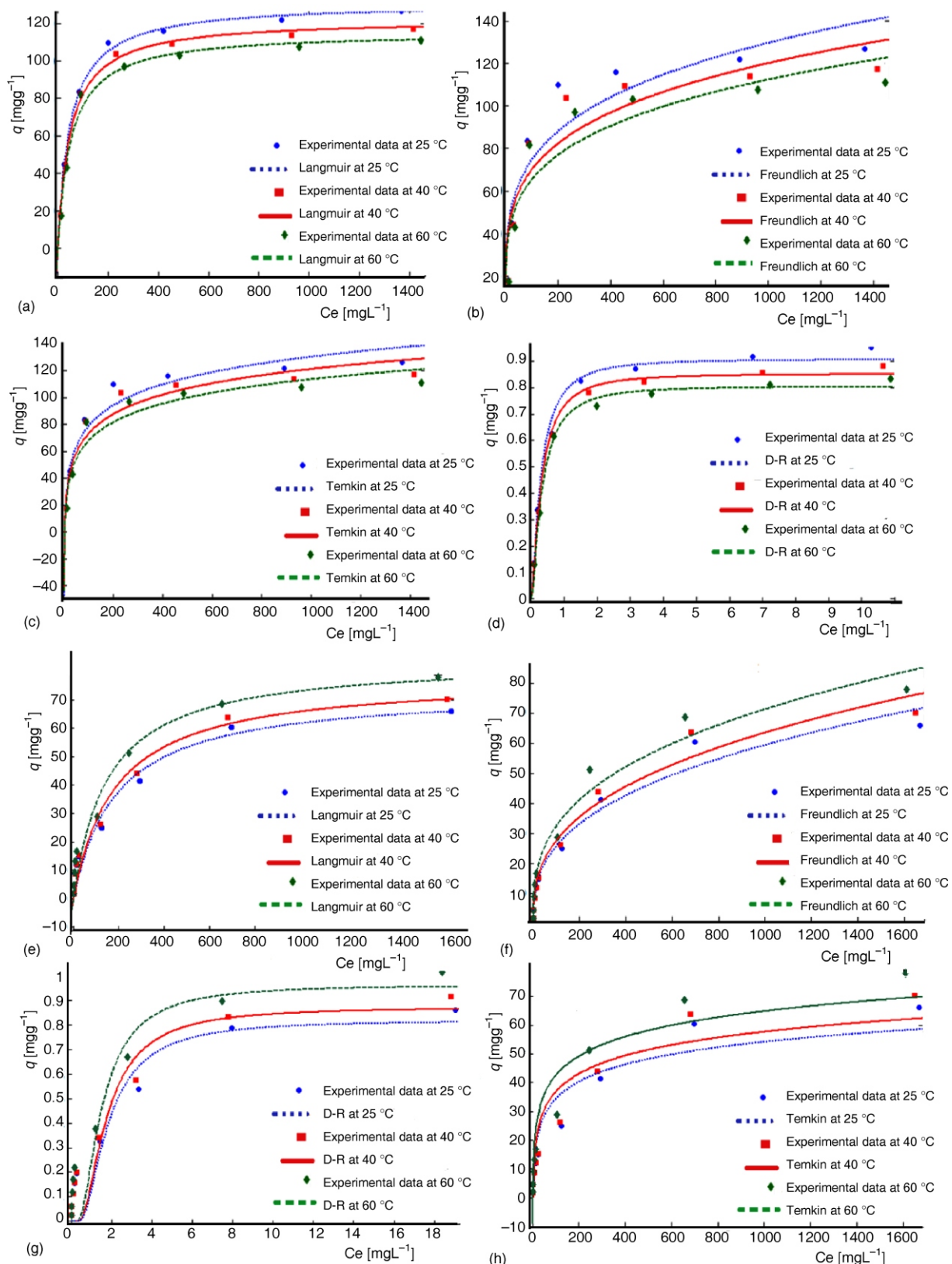


**Figure 8.** (a) Langmuir, (b) Freundlich, (c) Temkin and (d) D-R isotherms for adsorption Cs(I), and (e) Langmuir, (f) Freundlich, (g) Temkin and (h) D-R isotherms for adsorption of Sr(II) ions at 298, 313, and 333 K on modified zeolite

**Table 4. Sorption isotherm parameters of Cs(I) and Sr(II)**

Isotherms		298 K	313 K	333 K
D-R (Sr)	$q_{\max}$ [mmol $g^{-1}$ ]	0.8197	0.8727	0.9639
	$B_{DR}$ [mol $^2J^{-2}$ ]	6.20E-07	5.28E-07	3.75E-07
	$E_s$ [kJmol $^{-1}$ ]	0.898	0.972	1.155
	$R^2$	0.8838	0.8931	0.905
D-R (Cs)	$q_{\max}$ [mmol $g^{-1}$ ]	0.908	0.853	0.8057
	$B_{DR}$ [mol $^2J^{-2}$ ]	5.06E-08	4.75E-08	4.54E-08
	$E_s$ [kJmol $^{-1}$ ]	3.143	3.2420	3.320
	$R^2$	0.9872	0.9867	0.9861
Temkin (Sr)	$b_T$ [Jmol $^{-1}$ ]	289.6	287.8	286.9
	$K_T$ [Lmg $^{-1}$ ]	0.5601	0.5884	0.8263
	$R^2$	0.8935	0.8939	0.9097
Temkin (Cs)	$b_T$ [Jmol $^{-1}$ ]	110.7	124.9	139.6
	$K_T$ [Lmg $^{-1}$ ]	0.339	0.3375	0.3086
	$R^2$	0.9462	0.9331	0.9244
Freundlich (Sr)	$K_F$ [mgg $^{-1}$ ]	4.938	5.289	6.831
	$n$	0.3602	0.3599	0.3396
	$R^2$	0.9725	0.9724	0.9728
Freundlich (Cs)	$K_F$ [mgg $^{-1}$ ]	24.78	23.86	22.21
	$n$	0.2394	0.2339	0.2346
	$R^2$	0.8499	0.835	0.8286
Langmuir (Sr)	$q_m$ [mgg $^{-1}$ ]	130.8	122.2	83.94
	$K_L$ [Lmg $^{-1}$ ]	0.005339	0.005468	0.006675
	$R^2$	0.9836	0.9866	0.9925
Langmuir (Cs)	$q_m$ [mgg $^{-1}$ ]	73.22	77.81	115.3
	$K_L$ [Lmg $^{-1}$ ]	0.02067	0.02063	0.01945
	$R^2$	0.996	0.9936	0.9961

**AUTHORS' CONTRIBUTIONS**

The experiments were carried out by H. R. Mahmudian. The manuscript was written by T. Yousefi and the figures were prepared by H. R. Mahmudian and T. Yousefi. All authors analyzed and discussed the results.

**REFERENCES**

- [1] Jahangiri, H., High Efficient Nanocomposite for Removal of Heavy Metals (Hg $^{2+}$  and Pb $^{2+}$ ) from Aqueous Solution M. Ebadi, *Journal of Nanostructures*, 6 (2016), 1, pp. 23-27
- [2] Heidary, F., et al., Synthesis, Characterization and Transport Properties of Novel Ion-exchange Nanocomposite Membrane Containing In-situ Formed ZnO Nanoparticles, *Journal of Nanostructures*, 5 (2015), 4, pp. 319-325
- [3] Milani, M. H., I-V Characteristics of a Molecular Wire of Polyaniline (Emeraldine Base), *International Nanoscience and Nanotechnology*, 7 (2011), 4, pp. 201-204
- [4] Alireza, B., Mahroo K., Determination of Lead and Cadmium in Various Food Samples by Solid Phase Extraction Using a Novel Amino-Vinyl Functionalized Iron Oxide Magnetic Nanoparticles, *International Nanoscience and Nanotechnology*, 12 (2016), 2, pp. 91-101
- [5] Swati, S., Umesh, S., Development of Bimetal Oxide Doped Multifunctional Polymer Nanocomposite for Water Treatment, *International Nano Letters*, 6 (2016), 4, pp. 223-234
- [6] Farahmandjou, M., Golabiyan, N., Synthesis and Characterization of Alumina (Al $_2$ O $_3$ ) Nanoparticles Prepared by Simple Sol-Gel Method, *International Journal of Bio-Inorganic Hybrid Nanomaterials*, 5 (2016), pp. 73-77
- [7] Ahmadpour, A., et al., Performance of MWCNT and a Low-Cost Adsorbent for Chromium(VI) Ion Removal, *Journal of Nanostructure in Chemistry*, 4 (2014), 4, pp. 171-178
- [8] Rehakova, M., et al., Agricultural and Agrochemical Uses of Natural Zeolite of the Clinoptilolite Type, *Current Opinion in Solid State and Materials Science*, 8 (2004), 6, pp. 397-404
- [9] Apreutesei, R. E., et al., Surfactant-Modified Natural Zeolites for Environmental Applications in Water Purification, *Environmental Engineering and Management Journal*, 7 (2008), 2, pp. 149-161
- [10] Yousefi, T., et al., Abolfazl Aghaei, Cd(II) Sorption on Iranian Nano Zeolites: Kinetic and Thermodynamic Studies, *Journal of Water and Environmental Nanotechnology*, 1 (2016), 2, pp. 75-83
- [11] Deming, L. B., et al., The Sequestration of Sr(II) and Cs(I) from Aqueous Solutions by Magnetic Graphene Oxides, *Journal of Molecular Liquids*, 209 (2015), Sept., pp. 508-514
- [12] Susan, S., et al., Synthesis, Characterization and Application of Lanthanide Metal-Ion-Doped TiO $_2$ /Ben-

- tonite Nanocomposite for Removal of Lead (II) and Cadmium(II) from Aquatic, *Journal of Water and Environmental Nanotechnology*, 1 (2016), 1, pp. 35-44
- [13] Yousefi, T., et al., Sr(II) Sorption by Nano Clinoptilolites, (Afrazand, Abyaneh, Toska and Neginpowder): Kinetic, Thermodynamic and Mechanism Studies, *Materials Focus*, 5 (2016), 2, pp. 137-145
- [14] Yousefi, T., et al., Cerium(III) Molybdate Nanoparticles: Synthesis, Characterization and Radionuclides Adsorption Studies, *Journal of Hazardous Materials*, 215-216 (2012), May, pp. 266-271
- [15] Gomez-Aviles, A., et al., Zeolite-Sepiolite Nano-heterostructures, *Journal of Nanostructure in Chemistry*, 4 (2014), 90, pp. 82-90
- [16] Haas, P. A., A Review of Information on Ferrocyanide Solids for Removal of Cesium from Solutions, *Separation Science and Technology*, 28 (1993), 17-18, pp. 2479-2506
- [17] Okamura, Y., et al., Cesium Removal in Freshwater Using Potassium Cobalt Hexacyanoferrate-Impregnated Fibers, *Radiation Physics and Chemistry*, 94 (2014), 1, pp. 119-122
- [18] Watari, K., et al., Removal of Cesium Using Cobalt-Ferrocyanide-Impregnated Polymer-Chain-Grafted Fibers, *Journal of Nuclear Science and Technology*, 5 (1968), 1, pp. 309-312
- [19] Yousefi, T., et al., Potential Application of a Nanocomposite: HCNFe@Polymer for Effective Removal of Cs(I) from Nuclear Waste, *Progress in Nuclear Energy*, 85 (2015), Nov., pp. 631-639
- [20] Vincent, T., et al., Immobilization of Metal Hexacyanoferrate Ion-Exchangers for the Synthesis of Metal Ion Sorbents, A Mini-Review, *Molecules*, 20 (2015), 11, pp. 20582-20613
- [21] Munthali, M. W., et al., Cs<sup>+</sup> and Sr<sup>2+</sup> Adsorption Selectivity of Zeolites in Relation to Radioactive Decontamination, *Journal of Asian Ceramic Societies*, 3 (2015), May, pp. 245-250
- [22] Mozgawa, W., Bajda, T., Spectroscopic Study of Heavy Metals Sorption on Clinoptilolite, *Physics and Chemistry of Minerals*, 31 (2005), 10, pp. 706-713
- [23] Dizadji, N., et al., Experimental Investigation of Adsorption of Copper from Aqueous Solution Using Vermiculite and Clinoptilolite, *International Journal of Environmental Research*, 7 (2013), 4, pp. 887-894
- [24] Qing, Y., et al., Selective Sorption Mechanism of Cs<sup>+</sup> on Potassium Nickel Hexacyanoferrate(II) Compounds, *Journal of Radioanalytical and Nuclear Chemistry*, 304 (2015), 2, pp. 527-533
- [25] Smicklas, I., et al., Removal of Cs<sup>1+</sup>, Sr<sup>2+</sup>, and Co<sup>2+</sup> from Aqueous Solutions by Adsorption on Natural Clinoptilolite, *Applied Clay Science*, 35 (2007), 1-2, pp. 139-144
- [26] Doula, M. K., Synthesis of a Clinoptilolite-Fe System with High Cu Sorption Capacity, *Chemosphere*, 67 (2007), 4, pp. 731-740
- [27] Yousefi, T., et al., FeIII x SnII y SnIV1- x- y H n [P (Mo3O10)4] · xH<sub>2</sub>O New Nano Hybrid, for Effective Removal of Sr(II) and Th(IV), *Journal of Radioanalytical and Nuclear Chemistry*, 307 (2016), July, pp. 941-953
- [28] Huang, C., Cheng, W. P., Thermodynamic Parameters of Iron-Cyanide Adsorption Onto g-Al<sub>2</sub>O<sub>3</sub>, *Journal of Colloid and Interface Science*, 188 (1997), 2, pp. 270-274
- [29] Cole, T., et al., Diffusion Mechanism of Multiple Strontium Species in Clay, *Geochimica et Cosmochimica Acta*, 64 (2000), 3, pp. 385-396
- [30] Qi, H., et al., Removal of Sr(II) from Aqueous Solutions Using Polyacrylamide Modified Graphene Oxide Composites, *Journal of Molecular Liquids*, 208 (2015), Aug., pp. 394-401
- [31] Ofomaja, A. E., Intraparticle Diffusion Process for Lead(II) Biosorption Onto Mansonia Wood Sawdust, *Bioresource Technology*, 101 (2010), 15, pp. 5868-5876
- [32] Sarkar, S., et al., Kinetics and Mechanism of Fluoride Removal Using Laterite, *Industrial & Engineering Chemistry Research*, 45 (2006), 17, pp. 5920-5927
- [33] Cortes-Martinez, R., et al., Cesium Sorption by Clinoptilolite-Rich Tuffs in Batch and Fixed-Bed Systems, *Desalination*, 258 (2010), 1-3, pp. 164-170
- [34] Chandramouleeswaran, S., Ramkumar, J., n-Benzoyl-n-Phenylhydroxylamine Impregnated Amberlite XAD-4 Beads for Selective Removal of Thorium, *Journal of Hazardous Materials*, 280 (2014), Sept., pp. 514-523
- [35] Langmuir, I., The Adsorption of Gases on Plane Surfaces of Glass, Mica, and Platinum, *Journal of the American Chemical Society*, 40 (1918), 9, pp. 1361-1403
- [36] Yousefi, T., et al., Effective Removal of Ce(III) and Pb(II) by New Hybrid Nano-Material: HnPmo12O40@Fe(III)xSn(II)ySn(IV)1-x-y, *Process Safety and Environmental Protection*, 98 (2015), July, pp. 211-220
- [37] Freundlich, H., Over the Adsorption in Solution, *Z. Phys. Chem.*, 28 (1909), 25, pp. 385-470
- [38] Tempkin, M. I., Pyzhev, V., Kinetics of Ammonia Synthesis on Promoted Iron Catalyst, *Acta Phys. Chim., USSR* 12 (1940), May, pp. 327-356
- [39] Radushkevich, L. V., Dubinin, M. M., The Equation of the Characteristic Curve of Activated Charcoal, *Doklady Akademii Nauk S.S.S.R.*, 55 (1947), March, pp. 327-329
- [40] Rojas, G., et al., Adsorption of Azo-Dye Orange II from Aqueous Solutions Using a Metal-Organic Framework Material: Iron-Benzenetricarboxylate, *Materials*, 7 (2014), 12, pp. 8037-8057
- [41] Nabiollah, M., et al., Porosity, Characterization and Structural Properties of Natural Zeolite-Clinoptilolite as a Sorbent, *Environ. Prot. Eng.*, 39 (2013), 1, pp. 140-151

Received on October 2, 2016

Accepted on December 1, 2016

**Тахер ЈУСЕФИ, Хамид Реза МАХМУДИЈАН, Мејсам ТОРАБ-МОСТАЕДИ,  
Мохамад Али МУСАВИЈАН, Реза ДАВАРКАХ**

**УЧВРШЋАВАЊЕ СоНФС НАНОЧЕСТИЦА НА  
КЛИНОПТИЛОЛИТ РАДИ СМАЊЕЊА НУКЛЕАРНОГ ОТПАДА**

Извршено је таложeње кобалт фeроцијанида на клиноптилолит у својству неорганског полимера како би се побољшале његове механичке особине. Ради повећања могућности прихватања јона адсорбента, размотрена су два важна фактора: стабилност (зеолит) и велики капацитет адсорпције (кобалт фeроцијанид). Провера побољшања извршена је дифракцијом икс-зрачења, скенирајућим електронским микроскопом и Фурије-трансформисаном спектроскопијом у инфрацрвеној области. Побољшани зеолит употребљен је за уклањање јона Sr(II) и Cs(I) из воденог раствора у смеси. Капацитет адсорпције побољшаног зеолита за Cs(I) и Sr(II) повећан је на  $90 \text{ mgg}^{-1}$  и  $130 \text{ mgg}^{-1}$ , респективно. Уклањање Sr(II) и Cs(I) испитивано је у зависности од времена мешања, pH, почетне концентрације Sr(II) и Cs(I) и температуре. Експериментални подаци добро се поклапају са Лангмировим изотермним моделом за два сорбент јона метала. Подаци о временској зависности сорпције показују да је прихватање Cs (I) и Sr(II) веома брзо и да се видљива равнотежа постиже после 100 минута од тренутка контакта. Кинетички експериментални подаци фитовани су моделима функција псеудо првог и другог реда, дуплим експоненцијалним моделом, Еловичевим моделом и интрачестичним дифузионим моделом. Урађена је и процена брзина сорпција, капацитета и вредности константи.

*Кључне речи: природни зеолити, клиноптилолит, Cs(I), Sr(II), адсорпција, кобалт фeроцијанид, наночестица*

---